Numerical Assessment on the Influence of Engine Calibration Parameters on Innovative Piston Bowls Designed for Light-Duty Diesel Engines

energies

MDPI

Article

Numerical Assessment on the Influence of Engine Calibration Parameters on Innovative Piston Bowls Designed for Light-Duty Diesel Engines

Federico Millo [1], Andrea Piano [1,*], Salvatore Roggio [1], Francesco C. Pesce [2], Alberto Vassallo [2] and Andrea Bianco [3]

[1] Energy Department, Politecnico di Torino, 10129 Torino, Italy; federico.millo@polito.it (F.M.); salvatore.roggio@polito.it (S.R.)
[2] PUNCH Torino S.p.A., 10129 Torino, Italy; francesco_concetto.pesce@punchtorino.com (F.C.P.); alberto_lorenzo.vassallo@punchtorino.com (A.V.)
[3] POWERTECH Engineering S.r.l., 10127 Torino, Italy; a.bianco@pwt-eng.com
* Correspondence: andrea.piano@polito.it

Abstract: The optimization of the piston bowl design has been shown to have a great potential for air–fuel mixing improvement, leading to significant fuel consumption and pollutant emissions reductions for diesel engines. With this aim, a conventional re-entrant bowl for a 1.6 L light-duty diesel engine was compared with two innovative piston designs: a stepped-lip bowl and a radial-bumps bowl. The potential benefits of these innovative bowls were assessed through 3D-CFD simulations, featuring a calibrated spray model and detailed chemistry. To analyse the impact of these innovative designs, two different engine operating conditions were scrutinized, corresponding to the rated power and a partial load, respectively. Under the rated power engine operating condition, a start of injection sensitivity was then carried out to assess the optimal spray–wall interaction. Results highlighted that, thanks to optimal injection phasing, faster mixing-controlled combustion could be reached with both the innovative designs. Moreover, the requirements in terms of swirl were also investigated, and a higher swirl ratio was found to be necessary to improve the mixing process, especially for the radial-bumps design. Finally, at part-load operating conditions, different exhaust gas recirculation (EGR) rates were analysed for two injection pressure levels. The stepped-lip and radial-bumps bowls highlighted reduced indicated specific fuel consumption (ISFC) and soot emissions values over different rail pressure levels, guaranteeing NO_x control thanks to the higher EGR tolerance compared with the re-entrant bowl. The results suggested the great potential of the investigated innovative bowls for improving efficiency and reducing emissions, thus paving the way for further possible optimization through the combination of these designs.

Keywords: diesel engine; innovative piston bowl; computational fluid dynamics; additive-manufacturing-enabled design; stepped-lip bowl; radial-bumps bowl

Citation: Millo, F.; Piano, A.; Roggio, S.; Pesce, F.C.; Vassallo, A.; Bianco, A. Numerical Assessment on the Influence of Engine Calibration Parameters on Innovative Piston Bowls Designed for Light-Duty Diesel Engines. *Energies* **2022**, *15*, 3799. https://doi.org/10.3390/en15103799

Academic Editor: Constantine D. Rakopoulos

Received: 4 April 2022
Accepted: 18 May 2022
Published: 21 May 2022

1. Introduction

Nowadays, the design of a diesel engine combustion system requires a balance among multiple and conflicting drivers. The compliance with even more stringent emission regulations has to be reconciled with the need of improving fuel economy without deteriorating durability and reliability. In addition, the customer experience should be guaranteed, achieving the requirements in terms of vehicle performance while keeping the noise and vibration under control. Lastly, the effort of balancing these multiple tradeoffs is made even more difficult by the always compelling need for cost reduction. In this context, the selection of the market segment target can affect the relative weight of the abovementioned drivers. There are, indeed, several critical differences between light- and heavy-duty applications. On one side, the light-duty engines are mainly optimized in operating conditions

in which the spray is unable to deliver a proper turbulence level needed for efficient mixing, requiring a supply by additional turbulence sources (e.g., swirl motion). On the other side, heavy-duty engines usually work in high-load conditions, in which most of the energy needed for the air–fuel mixing is provided by the spray. In recent years, several designs have been developed for heavy-duty engines, increasing the interaction between the fuel sprays and the piston bowl walls, thus enhancing the air–fuel mixing.

Among the different designs recently developed, the stepped-lip bowl has been considered the main alternative to the conventional re-entrant bowl [1–5]. This concept was implemented by Mercedes Benz on the OM654 engine, highlighting great benefits in terms of efficiency and soot reduction [6]. In addition, Cornwell and Smith, having a JCB off-highway diesel engine as a case study, were able to reach the emissions legislation limits even without any aftertreatment system [1,7]. Specifically, in this design, a chamfered lip is added to split the fuel into two toroidal vortices, within the bowl and in the squish region, thus increasing the air–fuel mixing [8]. The improved mixing enables higher exhaust gas recirculation (EGR) to control the NO_x emissions, and in combination with higher injection pressure, allows significant soot mitigation to be achieved [9]. Considering a similar design, Busch et al. have analysed the combustion process at different injection timings in [10]. They concluded that a faster mixing-controlled combustion phase (i.e., the 50–90% of mass fraction burned) can be obtained. This enhanced combustion rate has shown a strong correlation with the formation of intense toroidal vortices due to the step design, as experimentally evaluated by means of the combustion image velocimetry (CIV) technique by Zha et al. in [11]. Lastly, the stepped-lip bowl highlighted the great potential in terms of soot reduction [3,12]. Indeed, the more uniform fuel distribution increases the soot oxidation rate in the late portion of the combustion process.

Considering the low-swirl heavy-duty diesel engines, the flame to-flame interaction for the typical open bowl shape [13] dramatically reduces the combustion rate and increases the soot formation [14]. Therefore, to minimize this effect, Volvo proposed the wave bowl [15], introducing radial bumps in the outer bowl rim where adjacent flames interact. Thanks to this novel design, the late-cycle mixing can be improved, providing benefits both in terms of efficiency and soot emissions [16]. The radial bumps drive the adjacent flames to collide with a more favourable angle, significantly reducing the formation of rich zones and enhancing the flame velocity of the so-called radial mixing zone (RMZ) toward the cylinder axis. Therefore, the air entrainment onto the flame can be improved. Additionally, after the end of injection, when the RMZ detaches from the wall, the trailing edge of the flame leads to higher air entrainment, resulting in a faster burn rate [16]. Thanks to the improved mixing process, a higher mixing-controlled combustion phase was highlighted with respect to a conventional open bowl shape, gaining up to +1% thermal efficiency [17]. Moreover, the wave bowl has shown a remarkable improvement in the soot–NOx tradeoff under different partial load operating conditions, providing up to 80% soot reduction [16]. Recently, a radial-bumps bowl was numerically assessed for a light-duty diesel engine [18]. In this case, the higher swirl ratio reduced the intensity of the RMZ propagation, while the high bowl re-entrance resulted in enhanced flame recirculation toward the piston centre as a tumbling vortex. In this study, the radial-bumps design led to a strong improvement of the mixing rate with respect to a conventional re-entrant design. At part-load engine operating conditions, this resulted in flat soot–NO_x and brake-specific fuel consumption (BSFC)–NO_x tradeoffs for different EGR rates, leading to −50% soot and −5% BSFC with respect to the re-entrant bowl [18].

Nowadays, the possibility to build up innovative piston designs thanks to steel-based additive manufacturing (AM) procedures has enabled high-complexity and undercut geometries for further geometrical optimization [19–21]. In this context, the potential synergies between the stepped-lip and the radial-bumps bowls were experimentally evaluated by Belgiorno et al. in [21]. In this study, a re-entrant sharp-stepped bowl and a number of radial bumps equal to the nozzle holes in the inner bowl rim were combined in a single-piston concept, highlighting an impressive soot reduction without any fuel consumption

penalties. A similar concept was also investigated by means of both numerical and optical techniques, showing enhanced air–fuel mixing [22].

Considering all the above, the present study aims to investigate the potential of two combustion systems, originally developed for the heavy-duty sector, in a light-duty diesel engine: one based on the stepped-lip bowl and the other featuring radial bumps in the outer bowl rim. Considering the different engine applications, a detailed investigation has been performed to highlight the potential benefits of the proposed innovative designs. In this regard, a sensitivity analysis over different engine calibration parameters has been performed providing additional insights about the needs of the proposed designs in terms of engine calibration. With this aim, 3D computational fluid dynamics (3D-CFD) simulations of the combustion process were carried out, following the already developed 1D-/3D-CFD coupling methodology presented in [23]. The impact of different calibration parameters on the proposed piston bowl designs (re-entrant, stepped-lip, and radial-bumps) was investigated for two engine operating conditions. Firstly, at full load, an injection timing and swirl ratio sensitivity analysis was carried out. Then, at partial load, different EGR rates at two rail pressure levels were considered, highlighting the potential benefits in terms of efficiency and pollutant emissions.

2. Case Study

2.1. Engine Test Case

The analysed engine is a 1.6 L light-duty diesel engine, whose main characteristics are highlighted in Table 1.

Table 1. Test engine main features.

Cylinders	4
Displacement	1.6 L
Bore × Stroke	79.7 mm × 80.1 mm
Compression ratio	16:1
Turbocharger	Single-Stage with Variable Geometry Turbine (VGT)
Fuel injection system	Common rail direct injection (CRDI) Max Rail Pressure 2000 bar
Maximum power	100 kW @ 4000 rpm
Maximum torque	320 Nm @ 2000 rpm

The baseline test engine features the conventional re-entrant piston bowl, as shown in Figure 1—left. Then, two innovative piston bowl designs were investigated: a stepped-lip (Figure 1—middle) and a radial-bumps (Figure 1—right) bowls. The stepped-lip piston bowl was designed following the geometrical items reported in [1]. The radial-bumps bowl was developed by having the re-entrant bowl as a basis and adding a number of radial bumps in the outer bowl rim equal to the injector nozzle holes, as shown in [15].

Figure 1. Isometric view of the piston bowl geometries: (**left**) re-entrant; (**middle**) stepped-lip; (**right**) radial-bumps.

The two novel pistons have the same bore and squish height as the re-entrant bowl. Then, the piston bowl curvature was adjusted to keep the compression ratio equal to the nominal value (i.e., 16:1). The resulting bowl profile on the centre of the sector geometry can be observed in Figure 2, while the dashed green line refers to the bump geometry

in the sector periphery. Moreover, the injector protrusion was not modified for each investigated design.

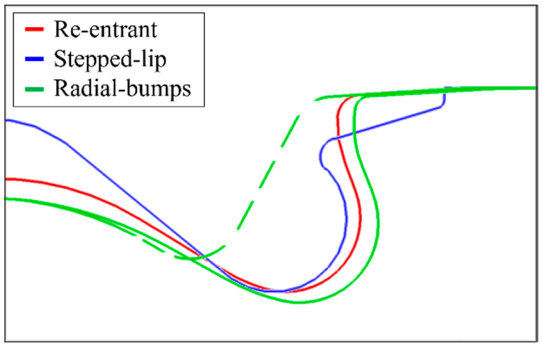

Figure 2. Piston bowl profiles.

The analysis was carried out considering two different engine operating conditions, one at part-load and one at rated power, as listed in Table 2. For these engine operating conditions, extensive validation of the numerical model for the re-entrant bowl was already presented in [23], highlighting fairly good agreement both in terms of the combustion process and emissions prediction.

Table 2. Selected engine working points.

Speed [rpm]	BMEP [bar]
1500	5.0
4000	18.5

2.2. Simulation Setup

The 1D-/3D-CFD coupling methodology, which has been developed and validated in [23], was adopted for the numerical simulations. The main steps of the methodology can be summarized as follows: The 1D-CFD complete engine model, developed in GT-SUITE and validated in [24], provides the time-dependent boundary conditions (i.e., thermodynamic and species concentration) for the first 3D-CFD simulation step. This latter, developed in CONVERGE CFD, is a cold flow simulation that was carried out for the analysis of the gas exchange process. Then, from the intake valve closure (IVC), the compression stroke and the combustion were investigated considering only a single sector of the full-cylinder geometry, which was centred along a single spray axis. For this simulation step, the injection rate profile was provided by the 1D-CFD injector model developed in [25,26]. In the last step, the 3D-CFD results were post-processed by means of GT-SUITE to guarantee the same solution methodology of the initial 1D-CFD engine model.

Regarding the 3D-CFD simulations, the Reynolds-averaged Navier–Stokes (RANS)-based renormalization group (RNG) k-ε model [27] was adopted. For the mesh refinement, the adaptive mesh refinement (AMR) technique, based on the velocity and temperature sub-grid criterion, was set [28]. The model settings in terms of mesh size, turbulence, and heat transfer models are listed in Table 3.

Table 3. Mesh size, turbulence, and heat transfer models.

Base grid	0.5 mm
Minimum grid	0.25 mm (fixed embedding and AMR)
Turbulence model	RNG k-ε model
Heat transfer model	O'Rourke and Amsden

For the spray model, the so-called "blob" injection method was considered and the breakup of droplets was modelled by means of a calibrated Kelvin Helmholtz and Rayleigh Taylor (KH-RT) model [29]. The spray sub-models are listed in Table 4.

Table 4. Spray sub-models.

Discharge coefficient model	Cv correlation [28]
Breakup model	Calibrated KH-RT
Turbulent dispersion	O'Rourke model [30]
Collision model	No Time Counter (NTC) collision [31]
Drop drag model	Dynamic drop drag [32]
Evaporation model	Frossling model [30]
Wall film model	O'Rourke [33]

For the combustion simulation, the detailed chemistry kinetic solver (SAGE) was adopted, considering the Skeletal Zeuch mechanism (121 species, 593 reactions) for the n-heptane oxidation [34]. This reaction mechanism includes the NO_x chemistry and the polycyclic aromatic hydrocarbons (PAH) soot precursor chemistry, thus enabling the particulate mimic (PM) model for the in-cylinder soot prediction [35–37].

3. Results and Discussion

3.1. Full Load Engine Operating Condition—4000 RPM × 18.5 Bar BMEP

3.1.1. Start of Injection Sensitivity

The injection timing plays a crucial role to maximize the potential benefits of a bowl design since the injection timing variation results in a different spray targeting which affect the near-wall flame behaviour. Therefore, the injection timing was swept at the rated power condition, keeping the injected fuel mass constant, considering the three different proposed designs. Three different starts of injection (SOIs) were investigated: the nominal SOI for the re-entrant bowl (baseline) and +5/+10 CAD with respect to the baseline SOI. The results of the SOI sweep in terms of mass fraction burned data (CA 10, 50, 75, 90) are shown in Figure 3a.

As expected, the early stages of the combustion process are not affected by the variation of the bowl design, as shown by CA10 data among the SOI sweeps. The innovative bowl designs start to influence the combustion process in the mixing-controlled combustion phase, as highlighted by the CA50 which is slightly advanced for both the stepped-lip and radial-bumps bowls. The CA75 shows even more evident differences: in fact, the innovative bowls show advanced combustion with respect to the re-entrant bowl for each SOI under investigation. During the late phase of the combustion process, the piston bowls highlight a different behaviour depending on the injection timing. The re-entrant shows the lowest sensitivity to the injection timing and the CA90 data are quite constant varying the SOI. Instead, the stepped-lip bowl highlights a remarkable increment of the CA90 by retarding the SOI. A similar result was experimentally assessed by Bush et al. in [10], in which the stepped-lip bowl highlighted for retarded SOI a strong increment of CA90 in comparison with a conventional re-entrant bowl. Indeed, in the late injection phase, the spray–wall impingement occurs above the step, causing poor air utilization within the bowl, as also reported in [18]. Regarding the radial-bumps bowl, a higher difference compared with the re-entrant design is observed for the baseline SOI. Then, moving to retarded SOI, the deviation from the CA90 of the re-entrant design is reduced. This suggests that the adoption of radial protrusions in the outer bowl rim provides higher benefits when optimal spray targeting is considered.

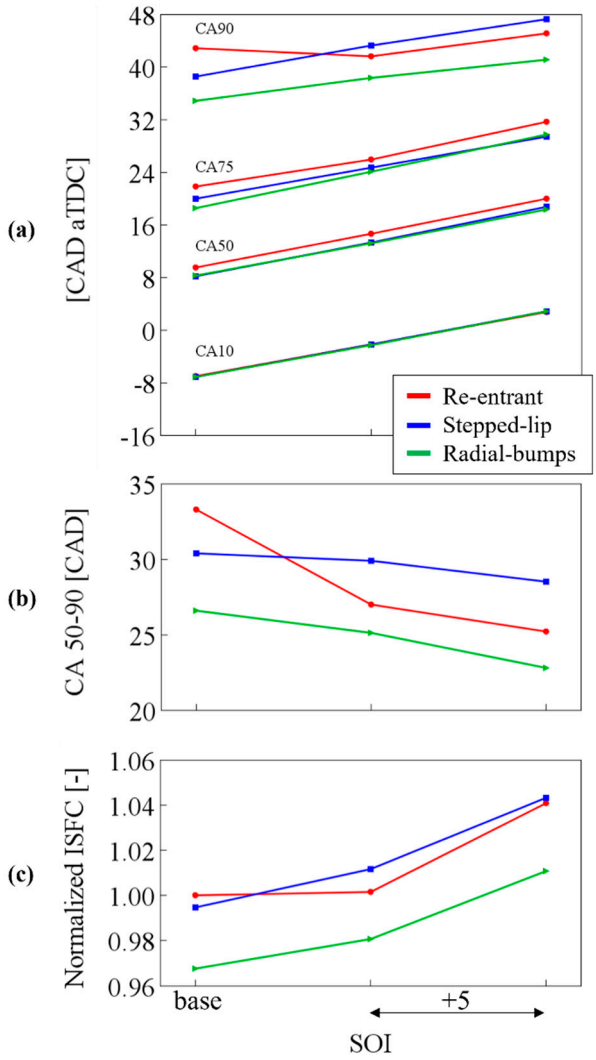

Figure 3. SOI sweep results. (**a**) Mass fraction burned data; (**b**) CA50-90; (**c**) ISFC normalized with respect to baseline engine configuration (bowl: re-entrant; SOI: base). Engine operating condition (baseline): 4000 RPM × 18.5 bar BMEP.

To better understand the injection timing sensitivity for each piston bowl under investigation, the duration of the last phase of the mixing-controlled combustion, represented by CA50-90, was further analysed as shown in Figure 3b. The radial-bumps bowl shows lower CA50-90 with respect to the re-entrant design for each investigated SOI. However, the higher deviation with respect to the re-entrant design can be observed for the nominal SOI, suggesting once again that a proper spray–wall interaction is required to enhance the radial-bumps benefits. When the stepped-lip design is adopted, retarding the SOI results in higher combustion duration in comparison with the other investigated designs due to the unbalanced fuel splitting on the step. Lastly, the ISFC normalized with respect to baseline engine configuration was investigated and it is depicted in Figure 3c. The radial-bumps bowl with the nominal SOI highlights the lowest ISFC, reaching a −3% reduction in comparison with the baseline re-entrant bowl. The highlighted potential improvement is comparable with the results obtained for a similar bowl design in a heavy-duty diesel engine application, as assessed by Zhang et al. in [17]. In this work, higher thermal efficiency (up to +1%) was experimentally assessed over different high-load engine operating conditions. Similar behaviour has been found considering the stepped-lip design at nominal SOI, with an ISFC reduction lower than 1%. Nevertheless, by retarding the SOI the stepped-lip bowl leads to

a worsening of ISFC with respect to the re-entrant bowl, confirming again the importance of a proper fuel split on the lip for an efficient combustion process.

To further analyse the injection timing impact on the combustion development among the piston bowls under investigation, the heat release rate (HRR) was scrutinized for two different SOIs (nominal and +10 CAD), as shown in Figure 4. For each investigated SOI, the premixed combustion stage is not significantly affected by the piston bowl design, confirming the results previously presented in Figure 3 (i.e., CA10). However, moving ahead in the combustion process, during the mixing-controlled phase, the re-entrant bowl shows a reduced HRR compared to the stepped-lip and radial-bumps designs. Indeed, considering the SOI_{base} (Figure 4—left), from −5 to +5 CAD aTDC, both the stepped-lip and the radial-bumps bowls lead to higher HRR. In this phase, indeed, the re-entrant bowl has shown the strongest jet-to-jet interaction and a reduced air–fuel mixing rate with respect to the other bowls [18]. From +5 CAD aTDC to the end of injection (EOI), the HRR for the stepped-lip bowl drops below the one obtained with the radial-bumps bowl. At this stage, the unbalanced fuel split on the step reduces the air utilization within the bowl slowing down the combustion process [18]. Conversely, the radial-bumps bowl shows the highest HRR at this stage, due to the improved air–fuel mixing rate thanks to the adoption of radial bumps [18]. Retarding the SOI (i.e., SOI_{base} +10 shown in Figure 4—right), as expected, the main injection premixed combustion is significantly attenuated. From +5 to +15 CAD aTDC, both the stepped-lip and the radial-bumps bowls show a higher combustion rate. However, moving ahead in the combustion the higher fuel in the squish region results in lower air utilization within the bowl, especially for the stepped-lip bowl, and the HRR reduces its intensity, even lower than the one obtained adopting the re-entrant bowl.

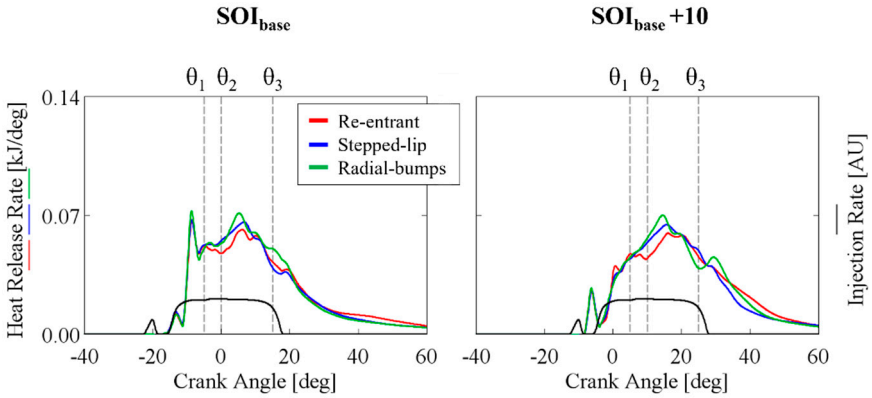

Figure 4. Heat release rate and injection rate profile: (**left**) SOI $_{base}$; (**right**) SOI $_{base}$ +10. Engine operating condition (baseline): 4000 RPM × 18.5 bar BMEP.

The combustion system behaviour for the two SOIs in Figure 4 was then further investigated by looking at the in-cylinder flame evolution. With this aim, the stoichiometric iso-surface contoured by temperature was considered representative of the flame front, as shown in Figures 5 and 6 for the SOI $_{base}$ and SOI $_{base}$ +10, respectively. The three different crank angles, θ_i, highlighted in Figure 4, are representative of the same degree interval after the start of injection to properly compare the different SOIs.

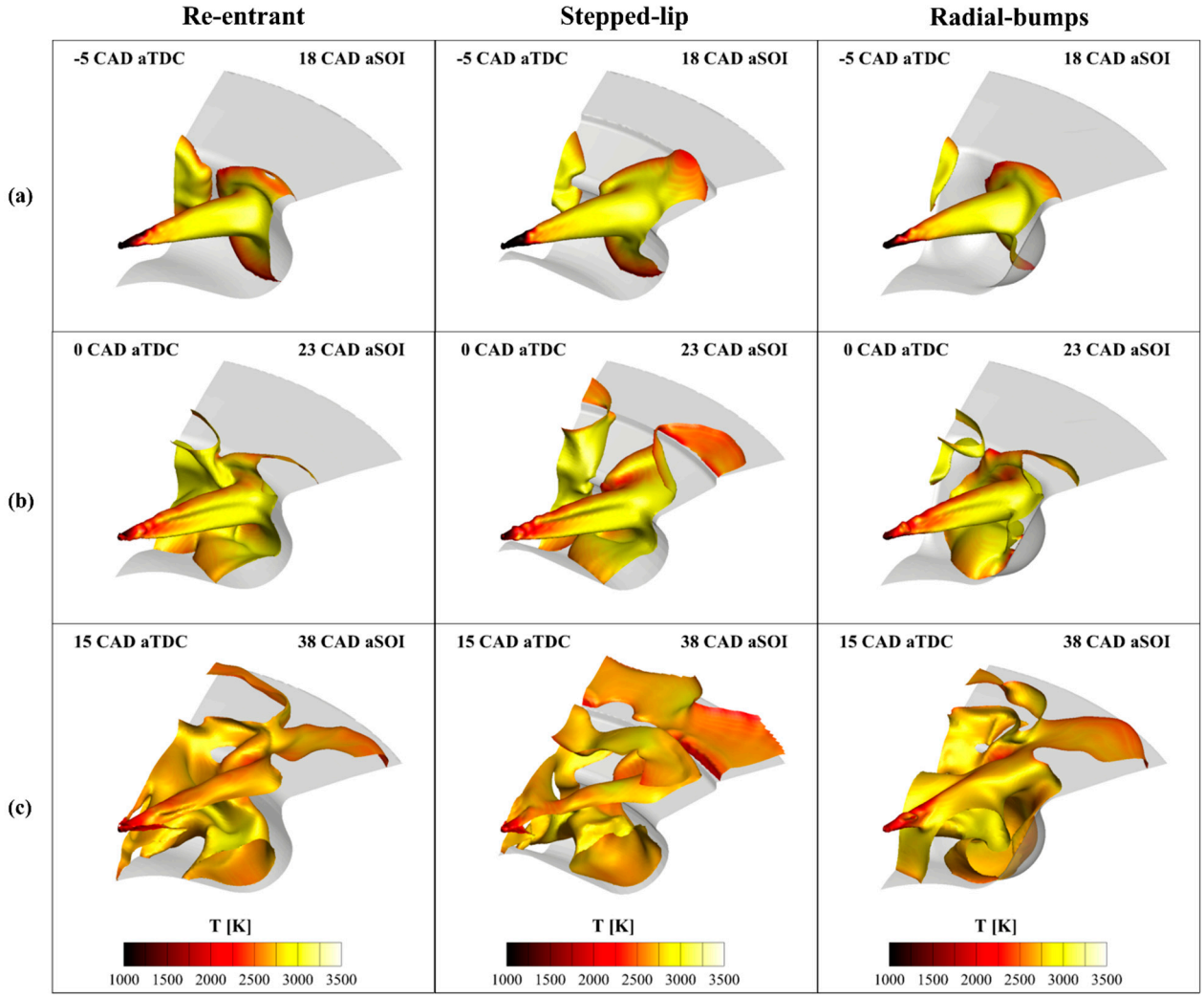

Figure 5. SOI $_{base}$: stoichiometric iso-surface contoured by temperature. (**a**) 18 CAD aSOI; (**b**) 23 CAD aSOI; (**c**) 38 CAD aSOI. (**left**) Re-entrant; (**middle**) stepped-lip; (**right**) radial-bumps. Engine operating condition (baseline): 4000 RPM × 18.5 bar BMEP.

- At θ_1 = +18 CAD aSOI
  At this stage, the flame/wall interaction plays the main role in the overall combustion rate. Considering the SOI $_{base}$, the re-entrant bowl highlights an HRR lower than the other bowls (see Figure 4) due to the interaction of adjacent flames, as shown in Figure 5a. Different mechanisms can be instead highlighted for the other designs under investigation. The stepped-lip bowl shows higher flame propagation above the step, increasing the air utilization in the squish area, while the radial-bumps bowl avoids the interaction of adjacent flames, increasing the combustion rate. Retarding the injection (SOI $_{base}$ +10, Figure 6a), all the bowls under investigation show similar results with respect to the baseline SOI due to the same piston position (−/+5 CAD aTDC) and thus similar spray–wall interaction. Therefore, even reducing the ignition delay, the re-entrant bowl shows the less intense HRR among the proposed designs, as already depicted in Figure 4.
- At θ_2 = +23 CAD aSOI
  Moving ahead in the engine cycle, the re-entrant bowl highlights a strong interaction between the adjacent flames for each SOI under investigation. This results in lower HRR compared with the other bowls (see Figure 4). Considering the SOI $_{base}$ (Figure 5b), the fuel split on the stepped-lip bowl allows a more even distribution of the flame downward within the bowl and upward in the squish region, improving

the air–fuel mixing [18]. Differently, in the radial-bumps bowl, the flames collision is significantly attenuated and the bumps coupled with the swirling flow enable a flow recirculation that improves the air–fuel mixing near the tip of the bump [18]. Retarding the SOI (SOI $_{base}$ +10, Figure 6b), similar results can be observed. Nevertheless, the more advanced piston position leads to higher flame recirculation in the squish area. This results in a reduced impact of the bump without completely jeopardizing its beneficial effect as a flames separator.

- At θ_3 = +38 CAD aSOI
  Near the EOI of the main injection event, the flame evolution is strongly dependent on the injection phasing. As shown in Figure 5c, at SOI $_{base}$, the stepped-lip bowl shows an intense flame redistribution above the step and the unbalanced split results in a lower combustion rate, as already highlighted in Figure 4. Retarding the SOI (SOI $_{base}$ +10, Figure 6c), all the piston bowl designs lead to a remarkable redistribution of the flame in the squish region. This effect is detrimental, especially for the radial-bumps bowl, where the reduced flame recirculation within the bowl leads to a lower impact of the bumps, providing a lower difference among the analysed SOIs than with the re-entrant design in terms of CA 50-90 (see Figure 3).

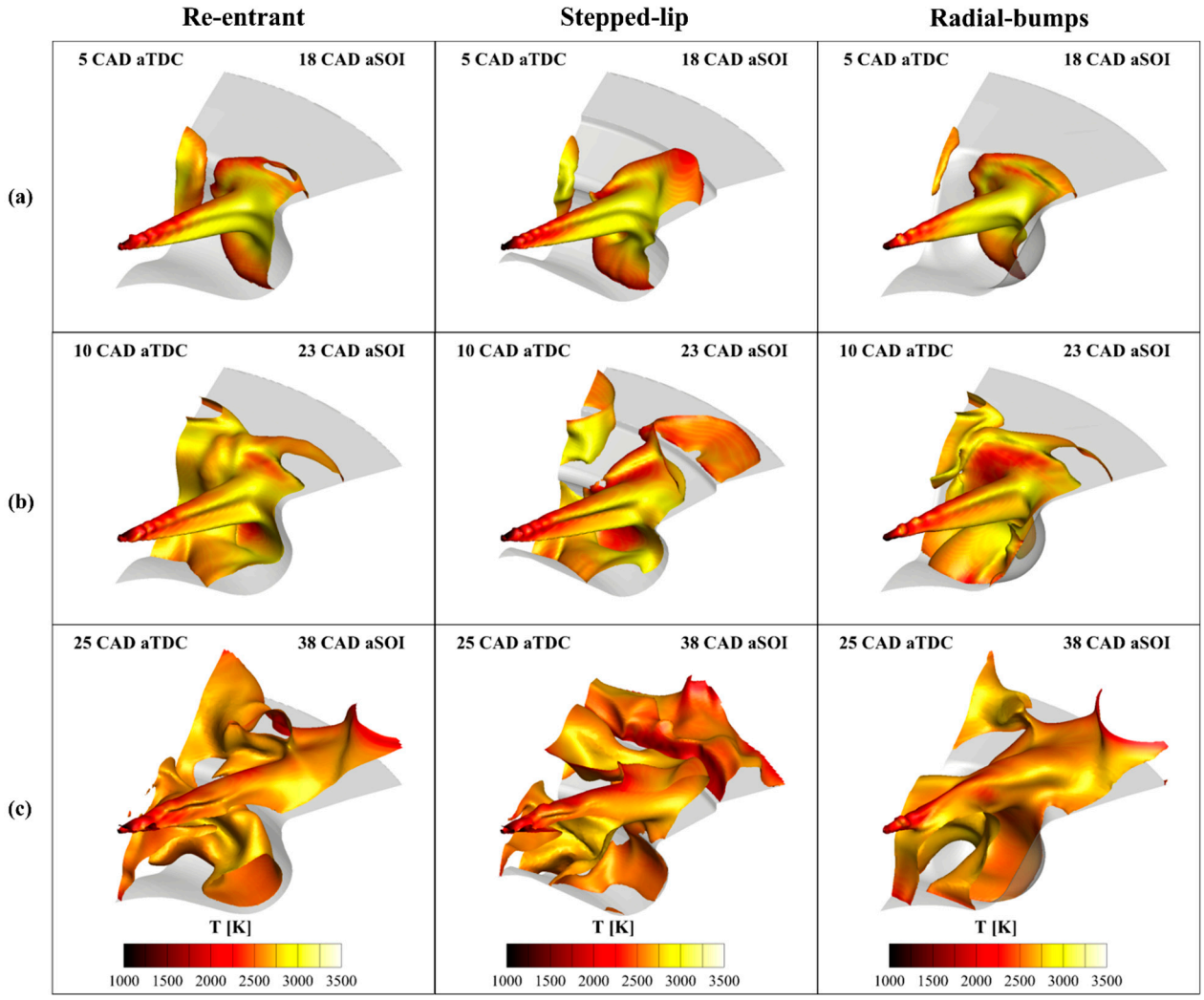

Figure 6. SOI $_{base}$ +10: stoichiometric iso-surface contoured by temperature. (**a**) 18 CAD aSOI; (**b**) 23 CAD aSOI; (**c**) 38 CAD aSOI. (**left**) Re-entrant; (**middle**) stepped-lip; (**right**) radial-bumps. Engine operating condition (baseline): 4000 RPM × 18.5 bar BMEP.

3.1.2. Swirl Ratio Sensitivity

The swirl ratio impact on the proposed combustion chamber has been already investigated under nonreacting conditions considering the full-cylinder geometry [18]. It is worth recalling that the stepped-lip bowl highlighted a lower swirl amplification than the re-entrant bowl due to the reduced squish flow intensity. Differently, the radial-bumps bowl showed an intense swirl collapse due to the bumps that can break the swirling flow, thus resulting in higher turbulent kinetic energy within the bowl [18]. To further understand the swirl impact on the combustion process, a swirl ratio at the IVC equal to zero (hereafter "zeroed") was imposed, zeroing the velocity components perpendicular to the cylinder axis. The HRR and the cumulative heat release (HR) for each investigated swirl ratio (i.e., nominal and zero) and combustion system are reported in Figure 7.

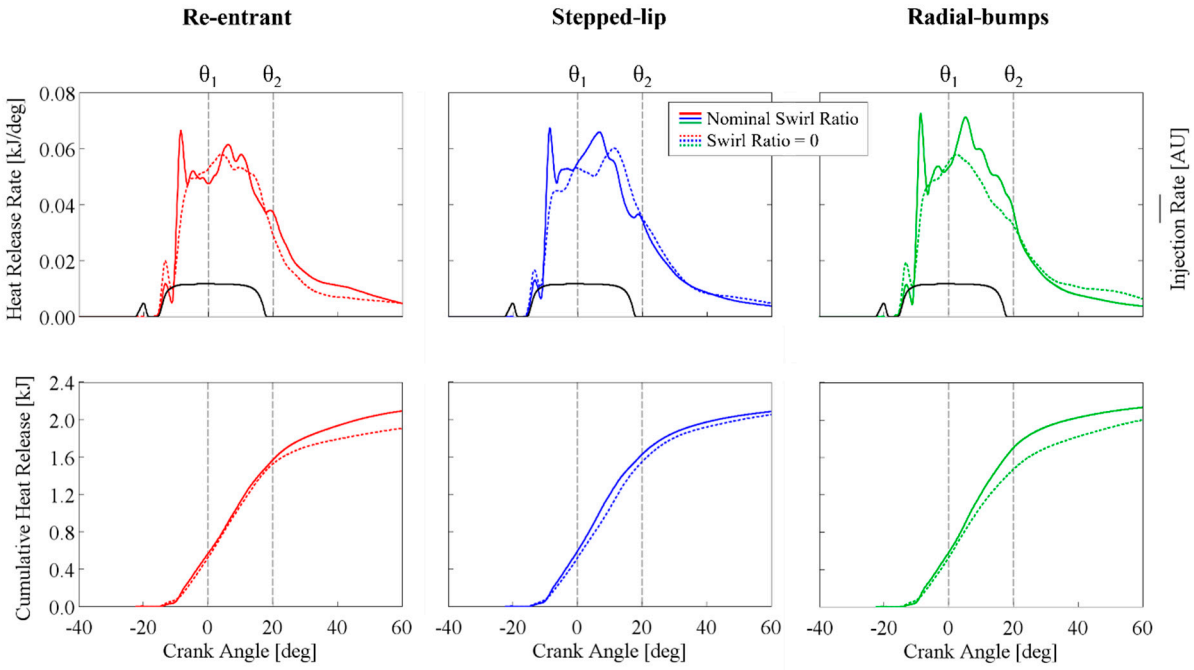

Figure 7. Swirl ratio results. (**top**) Heat release rate and injection rate; (**bottom**) cumulative heat release. (**left**) Re-entrant; (**middle**) stepped-lip; (**right**) radial-bumps. Engine operating condition (baseline): 4000 RPM × 18.5 bar BMEP.

For each combustion system under investigation, the zeroed swirl ratio leads to reduced air–fuel mixing during the pilot injection event, thus minimizing the over-leaning of the fuel jet and resulting in more intense pilot combustion. Due to that, the premixed combustion intensity of the main injection is reduced. Among the investigated piston geometries, the stepped-lip bowl is less affected by the swirl ratio variation due to its wider geometry, whose main flow structures are the toroidal vortices in the cylinder axis plane. Instead, the cumulative HR with the re-entrant and the radial-bumps designs appears significantly affected by the swirl ratio. In particular, the re-entrant design has comparable HR with and without swirling flow up to the EOI of the main event. After that, the zeroed swirl ratio reduces the air–fuel mixing of the residual fuel in the late cycle, and consequently, the cumulative HR drops down. The HRR for the radial-bumps bowl is significantly reduced during the injection event in the case of a null swirl ratio. Therefore, since the radial bumps tend to break the organized swirling motion [18], the radial-bumps bowl requires a higher swirl ratio to increase the air–fuel mixing rate and achieve a more efficient combustion process.

The equivalence ratio distribution was investigated to further understand the flow structures induced by the different swirl ratios for each combustion system under investigation. Two cutting planes were selected to show the numerical results: the spray axis

plane and the cylinder axis plane. The equivalence ratio contour plot for the selected planes and the isoline at the constant temperature equal to 1500 K (black line), which was selected as representative of the flame front, are shown in Figure 8 for the nominal swirl ratio and in Figure 9 for the zeroed swirl ratio.

Regarding the nominal swirl ratio, at TDC (Figure 8a), the re-entrant bowl shows an intense flame-to-flame interaction, while both the stepped-lip and radial-bumps bowls reduce this counterproductive effect, as already depicted in Figure 5. The stepped-lip bowl highlights higher flame propagation upward above the step, reducing the flame propagation in the tangential direction and thereby the collision of two adjacent flames. Instead, the radial-bumps bowl provides not only a reduced flame-to-flame interaction but also a different tangential flame propagation along the bowl surface. In particular, the swirling flow induces an asymmetrical spray–wall interaction and the fuel is driven by the bump into the consecutive sector, where the high air content enhances the air–fuel mixing. Considering the absence of swirl motion (Figure 9a), a symmetric spray–wall interaction is observed for all the investigated geometries, creating a more pronounced radial-mixing zone (RMZ) in the collision area of two adjacent flames, for the re-entrant and radial-bumps bowls. Nevertheless, for the radial-bumps bowl, the behaviour of the RMZ is significantly affected by the geometry of the bump, as also shown in [16]. The fuel plumes are driven by the bumps tip toward the cylinder centre where the available oxygen improves the air–fuel mixing onto the flame front. However, the intensity of this recirculation is high only in the upper-bump region, while in the bottom-bump region the tumbling vortex is the main flow structure due to the high bowl re-entrance [18]. Therefore, the radial-bumps bowl provides a more efficient air–fuel mixing with the nominal swirl ratio, since the bumps coupled with higher swirling flow enable beneficial flow structures.

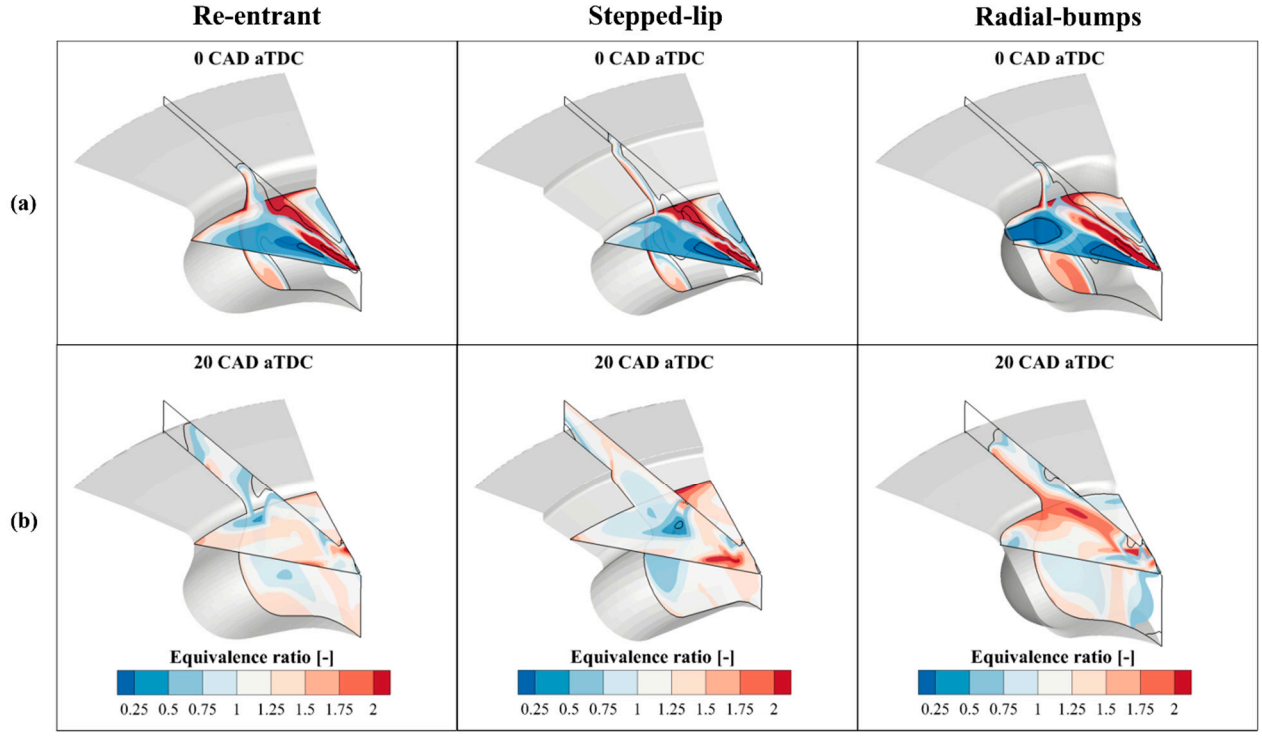

Figure 8. Nominal swirl ratio: equivalence ratio contour plot on the spray axis and cylinder axis planes. Black line: the constant temperature at 1500 K. (**a**) 0 CAD aTDC; (**b**) 20 CAD aTDC. (**left**) Re-entrant; (**middle**) stepped-lip; (**right**) radial-bumps. Engine operating condition (baseline): 4000 RPM × 18.5 bar BMEP.

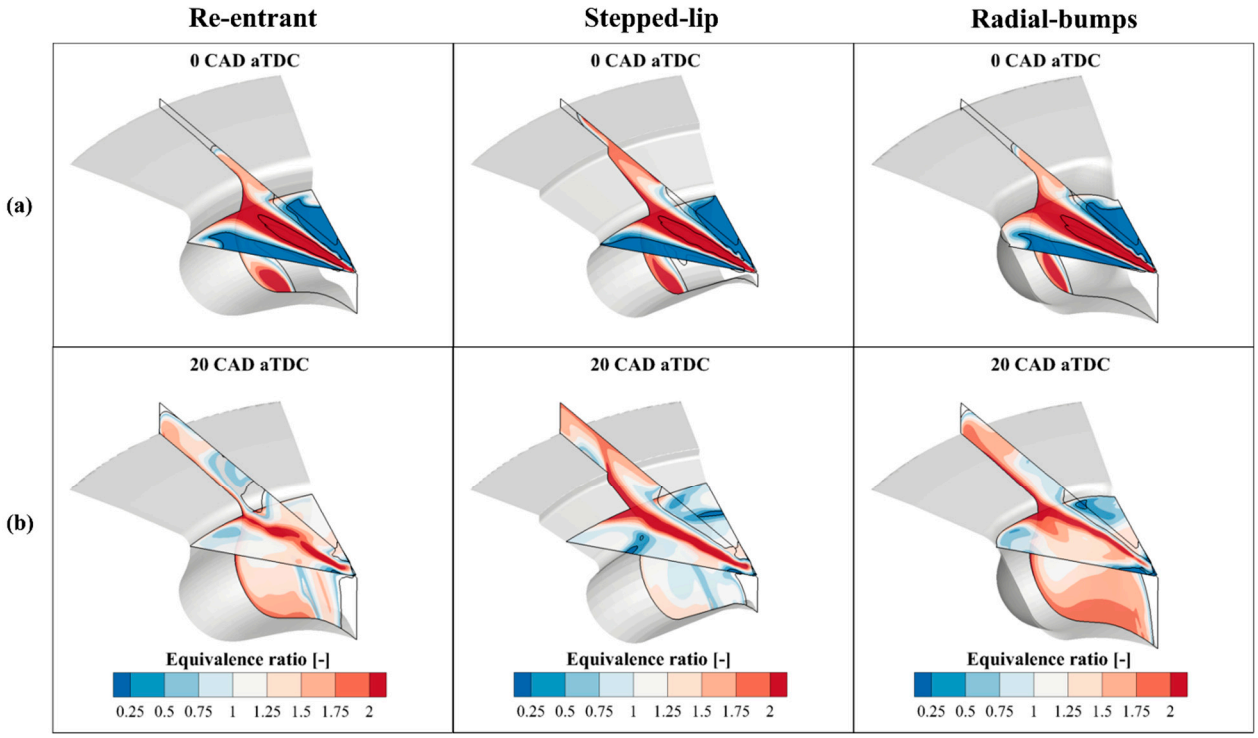

Figure 9. Zeroed swirl ratio: equivalence ratio contour plot on the spray axis and cylinder axis planes. Black line: the constant temperature at 1500 K. (**a**) 0 CAD aTDC; (**b**) 20 CAD aTDC. (**left**) Re-entrant; (**middle**) stepped-lip; (**right**) radial-bumps. Engine operating condition (baseline): 4000 RPM × 18.5 bar BMEP.

After the EOI of the main event (+20 CAD aTDC), the overall air–fuel mixing of the re-entrant bowl is significantly affected by the swirl ratio. At this stage with the nominal swirl ratio (Figure 8b), an almost homogeneous equivalence ratio toward the stoichiometric value can be observed, while removing the swirling flow (Figure 9b) the fuel-rich zones are still significant. This residual fuel is slowly oxidized, resulting in lower HRR in the late cycle, as shown in Figure 7. For the stepped-lip bowl, the equivalence ratio distribution within the bowl is comparable among the two tested swirl ratios. Indeed, the air–fuel mixing is mainly driven above the step which is slightly affected by the swirling flow. As a consequence, small differences can be observed in the late-cycle HRR considering different swirl ratios. Regarding the radial-bumps bowl, the bumps coupled with a higher swirl ratio continue to play a fundamental role on air–fuel mixing, leading to a more homogeneous mixture in the late-cycle with respect to the zeroed swirl ratio condition.

To globally characterize the effect of different swirl ratios on the combustion process at +20 CAD aTDC, the whole cylinder mass was binned by equivalence ratio into ten intervals, for both the nominal and the zeroed swirl ratio, as highlighted in Figure 10. For each piston bowl, the nominal swirl ratio shows the mode of the distribution closer to the stoichiometric range, while a lower cylinder mass fraction is shown in the tails of the distribution, suggesting a faster and more efficient combustion process. Nevertheless, only the radial-bumps bowl shows a strong sensitivity to the swirl ratio. Indeed, with the nominal swirl ratio, a higher cylinder mass fraction can be observed in the 0.8–1.2 equivalence ratio range, increasing the mixture homogeneity towards the stoichiometric value.

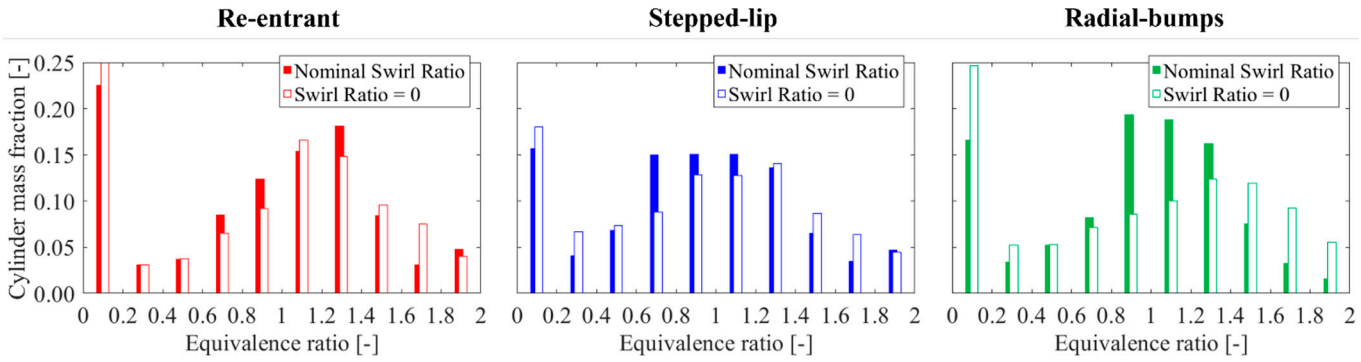

Figure 10. Equivalence ratio bins distribution for nominal and null swirl ratio at +20 CAD aTDC. (**left**) Re-entrant; (**middle**) stepped-lip; (**right**) radial-bumps. Engine operating condition (baseline): 4000 RPM × 18.5 bar BMEP.

3.2. Partial Load Engine Operating Condition—1500 RPM × 5.0 bar BMEP

EGR and Rail Pressure Sensitivity

At the partial load engine working point, different EGR rates and rail pressure levels were considered to assess the combustion system sensitivity in terms of fuel consumption and emissions. Three EGR rates were analysed: the baseline EGR for the re-entrant bowl and +/−5% with respect to the baseline EGR. The EGR rate was modified by varying the gas species concentration, evaluating only the different dilution and thermal effects thus keeping the same volumetric efficiency. Then, for each EGR rate, two rail pressure levels were considered (i.e., baseline and 50% higher than the baseline). The injection profile referred to the higher rail pressure was obtained by means of the injector model described in [25,26]. For each investigated calibration, the energizing time of the main injection was varied to keep the engine load equal to the one obtained for the baseline configuration (i.e., re-entrant bowl–nominal EGR–nominal rail pressure).

Figure 11 shows the EGR and rail pressure sweep analysis results in terms of ISFC, indicated specific NO_x ($ISNO_x$) and soot, each of them normalized with respect to the value of the baseline engine configuration. Starting from the ISFC under the nominal rail pressure (solid lines of Figure 11a), both the stepped-lip and the radial-bumps bowls highlight a reduced ISFC with respect to the re-entrant bowl (−1% and −4% at baseline EGR, respectively). Interestingly, going towards higher EGR rates, a further reduction in ISFC compared with the re-entrant bowl can be appreciated for both the innovative bowls, suggesting higher EGR tolerance due to the improved mixing process. As already assessed in [18], the radial-bumps design highlights a faster combustion process and the resulting higher temperature leads to higher NO_x production, as also confirmed in Figure 11b. Nevertheless, a further increase in the EGR rate can be adopted for NO_x mitigation due to the improved EGR tolerance. This is possible thanks to the impressive soot reduction highlighted by the stepped-lip and radial-bumps bowls with respect to the re-entrant design (−40% and −60% at baseline EGR), as shown in Figure 11. Additionally, it is worth noting that the radial-bumps bowl shows a flat trend over the EGR sweep, confirming that a higher EGR rate can be used for NOx mitigation even without soot penalties. This result is in line with the flatness of the soot–NOx tradeoff observed for a heavy-duty diesel engine application that features a similar bowl design [16], confirming the great potential of radial bumps on soot reduction.

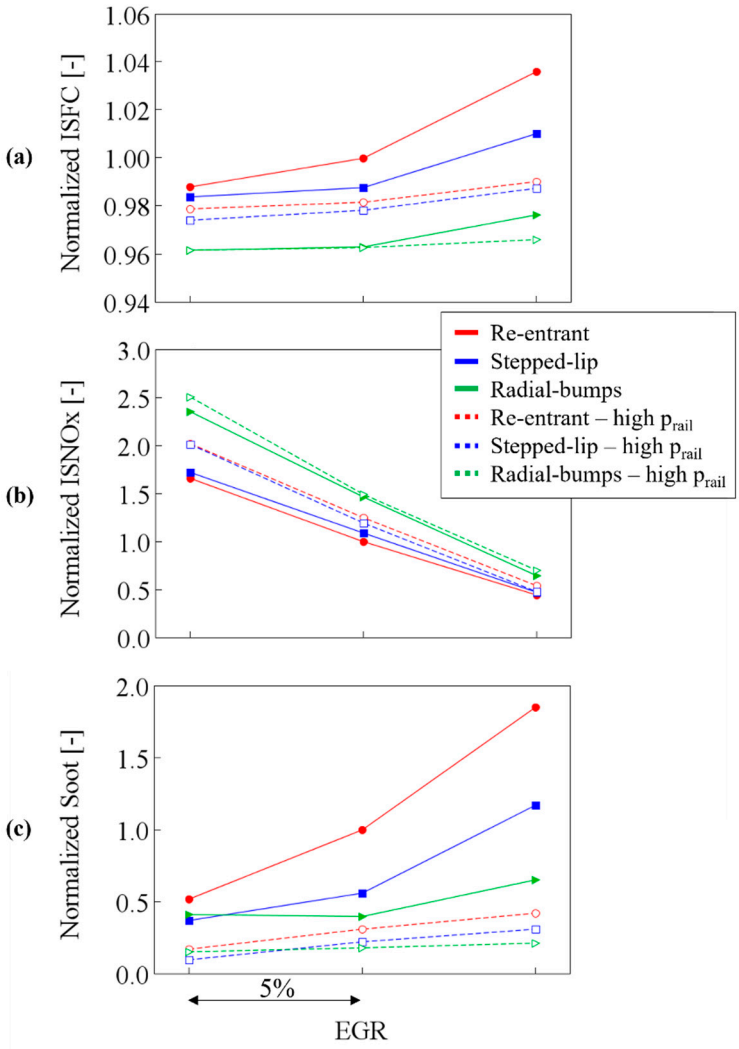

Figure 11. EGR and rail pressure sweep. (**a**) ISFC; (**b**) ISNO$_x$; (**c**) soot normalized with respect to baseline engine configuration. Engine operating condition: 1500 RPM × 5.0 bar BMEP.

Once we assessed the combustion systems sensitivity over different EGR rates, the rail pressure was increased with respect to the nominal condition (+50%) and the results for the higher rail pressure are reported in Figure 11 with dashed lines. As expected, increasing the rail pressure, a further improvement of the ISFC can be observed for all the investigated geometries due to the more intense premixed combustion phase. Nevertheless, the radial-bumps bowl with the baseline rail pressure still shows lower ISFC than the other bowls with higher rail pressure. Moreover, the enhanced premixed combustion phase leads to higher flame temperature, thus increasing the NO_x formation. However, the radial-bumps bowl highlights the lowest NO_x increment with respect to the baseline rail pressure. As far as soot emissions are concerned, the higher rail pressure results in a remarkable reduction thanks to the enhanced spray atomization that limits the soot formation for each investigated design. Interestingly, at baseline EGR, the re-entrant bowl with higher rail pressure shows comparable soot than with the radial-bumps bowl at baseline rail pressure. Then, the reduction in soot achievable by increasing the rail pressure in the conventional re-entrant design could be reached in the radial-bumps bowl thanks to the improved mixing, thus avoiding any worsening in parasitic losses due to the increased power demand of the high-pressure fuel pump.

4. Conclusions

This work aims to assess through numerical simulations the influence of different engine calibration parameters on the combustion process considering three piston bowl designs for a light-duty diesel engine. The baseline re-entrant design was compared with two innovative designs, originally developed for heavy-duty applications, named stepped-lip and radial-bumps bowl. Two operating conditions were considered at high and low engine load. Firstly, under the rated power condition, the optimal injection timing and swirl ratio were identified. Then, at the partial load operating point, an EGR sensitivity at two different rail pressure levels was carried out to assess the impact on engine efficiency and emissions. The main outcomes of this work can be summarized as follows.

First of all, both innovative designs showed high potential in improving the combustion process highlighting significant benefits in terms of indicated specific fuel consumption (ISFC) reduction in comparison with the conventional re-entrant geometry. This result is more evident for the radial-bumps design, thanks to which -3% and -4% ISFC reductions were achieved at full load and at partial load, respectively. Instead, for the stepped-lip bowl, a reduced improvement of the ISFC (-1%) was observed for two investigated operating conditions. In addition, the adoption of the stepped-lip or the radial-bumps designs led to a noticeable air–fuel mixing enhancement, thus halving the soot emissions in almost all the analysed operating conditions.

Several sensitivity analyses were carried out to clearly highlight the potential of the proposed combustion systems.

- As far as the start of injection (SOI) is concerned, the geometry modifications to enhance the mixing led to a higher impact on the injection timing due to the strong spray targeting sensitivity. This effect has been clearly highlighted for the stepped-lip design, in which the strong unbalanced fuel split toward the squish region, resulting in a less efficient combustion process.
- The analysis of the swirl ratio has clarified significant insights about the need for the proposed combustion systems in a light-duty engine. In fact, on one side, the stepped-lip bowl showed a slight impact of the swirl on the combustion rate, since the mixing process is mainly driven by the two toroidal vortices due to the fuel split on the step. On the other side, differently from the heavy-duty requirements, the radial-bumps design in combination with the swirling motion enables an efficient recirculation of the fuel, remarkably improving the air–fuel mixing rate.
- The analysis at different EGR rates has demonstrated the effect of the improved air–fuel mixing. Higher EGR tolerance was achieved, significantly reducing the soot emission and almost flattening the NOx–soot tradeoff, without any detrimental impact on the engine efficiency. In particular, at baseline EGR, -40% and -60% soot reductions were obtained by the stepped-lip and radial-bumps bowls, respectively.

Future analysis will be focused on further geometrical optimization with the aim to combine the potential benefits of these innovative profiles in terms of combustion and pollutant emissions.

Author Contributions: Conceptualization, F.M., A.P., F.C.P. and A.V.; methodology, A.P., S.R. and A.B.; validation, A.P. and S.R.; formal analysis, A.P., S.R. and A.B.; investigation, A.P., S.R. and A.B.; writing—original draft preparation, A.P. and S.R.; writing—review and editing, F.M., F.C.P., A.V. and A.B.; supervision, F.M., F.C.P. and A.V.; project administration, F.M. and F.C.P.; funding acquisition, F.M. All authors have read and agreed to the published version of the manuscript.

Funding: This research received no external funding.

Acknowledgments: Computational resources were provided by HPC@POLITO, a project of Academic Computing within the Department of Control and Computer Engineering at the Politecnico di Torino (http://www.hpc.polito.it). The authors would like to acknowledge General Motors (GM) and PUNCH Torino for their invaluable support to the research activity.

Conflicts of Interest: The authors declare no conflict of interest.

Abbreviations

AM	additive manufacturing
AMR	adaptive mesh refinement
BMEP	brake mean effective pressure
BSFC	brake-specific fuel consumption
CA10	crank angle at 10% of burned mass fraction
CA50	crank angle at 50% of burned mass fraction
CA50-90	duration for 50-90% of burned mass fraction
CA75	crank angle at 75% of burned mass fraction
CA90	crank angle at 90% of burned mass fraction
CAD aSOI	crank angle degrees after start of injection
CAD aTDC	crank angle degrees after top dead centre
CFD	computational fluid dynamics
CIV	combustion image velocimetry
CRDI	common rail direct injection
EGR	exhaust gas recirculation
EOI	end of injection
HR	heat release
HRR	heat release rate
ISFC	indicated specific fuel consumption
ISNOx	indicated specific NOx
IVC	intake valve closure
KH-RT	Kelvin Helmholtz and Rayleigh Taylor
NTC	no time counter
PAH	polycyclic aromatic hydrocarbons
PM	particulate mimic
RANS	Reynolds-averaged Navier–Stokes
RMZ	radial mixing zone
RNG	renormalization group
SOI	start of injection
TDC	top dead centre
VGT	variable geometry turbine

References

1. Cornwell, R.; Conicella, F. Direct Injection Diesel Engines, Ricardo UK Limited, West Sussex (GB). U.S. Patent 8770168 B2, 8 July 2014.
2. Styron, J.; Baldwin, B.; Fulton, B.; Ives, D.; Ramanathan, S. Ford 2011 6.7L Power Stroke® Diesel Engine Combustion System Development. In Proceedings of the SAE 2011 World Congress & Exhibition, Detroit, MI, USA, 12–14 April 2011; SAE Technical Paper 2011-01-0415. [CrossRef]
3. Yoo, D.; Kim, D.; Jung, W.; Kim, N.; Lee, D. Optimization of Diesel Combustion System for Reducing PM to Meet Tier4-Final Emission Regulation without Diesel Particulate Filter. In Proceedings of the SAE/KSAE 2013 International Powertrains, Fuels & Lubricants Meeting, Seoul, Korea, 21–23 October 2013; SAE Technical Paper 2013-01-2538. [CrossRef]
4. Kogo, T.; Hamamura, Y.; Nakatani, K.; Toda, T.; Kawaguchi, A.; Shoji, A. High Efficiency Diesel Engine with Low Heat Loss Combustion Concept-Toyota's Inline 4-Cylinder 2.8-Liter ESTEC 1GD-FTV Engine. In Proceedings of the SAE 2016 World Congress and Exhibition, Detroit, MI, USA, 12–14 April 2016; SAE Technical Paper 2016-01-0658. [CrossRef]
5. Lückert, P.; Arndt, S.; Duvinage, F.; Kemmner, M.; Binz, R.; Storz, O.; Reusch, M.; Braun, T.; Ellwanger, S. The New Mercedes-Benz 4-Cylinder Diesel Engine OM654–The Innovative Base Engine of the New Diesel Generation. In Proceedings of the 24th Aachen Colloquium Automobile and Engine Technology, Aachen, Germany, 5–7 October 2015; pp. 867–892.
6. Eder, T.; Kemmner, M.; Lückert, P.; Sass, H. OM 654–Launch of a New Engine Family by Mercedes-Benz. *MTZ Worldw.* **2016**, *77*, 60–67. [CrossRef]
7. Smith, A. Ricardo Low Emissions Combustion Technology Helps JCB Create the off-Highway Industry's Cleanest Engine. Ricardo Press Release. 2010. Available online: https://ricardo.com/news-and-media/news-and-press/ricardo-low-emissions-combustion-technology-helps (accessed on 20 May 2022).
8. Busch, S.; Zha, K.; Perini, F.; Reitz, R.; Kurtz, E.; Warey, A.; Peterson, R. Bowl Geometry Effects on Turbulent Flow Structure in a Direct Injection Diesel Engine. In Proceedings of the International Powertrains, Fuels & Lubricants Meeting, Heidelberg, Germany, 17–19 September 2018; SAE Technical Paper 2018-01-1794. [CrossRef]

9. Millo, F.; Piano, A.; Paradisi, B.P.; Boccardo, G.; Mirzaeian, M.; Arnone, L.; Manelli, S. The Effect of Post Injection Coupled with Extremely High Injection Pressure on Combustion Process and Emission Formation in an Off-Road Diesel Engine: A Numerical and Experimental Investigation. In Proceedings of the 14th International Conference on Engines & Vehicles, Naples, Italy, 15–19 September 2019; SAE Technical Paper 2019-24-0092. [CrossRef]
10. Busch, S.; Zha, K.; Kurtz, E.; Warey, A.; Peterson, R. Experimental and Numerical Studies of Bowl Geometry Impacts on Thermal Efficiency in a Light-Duty Diesel Engine. In Proceedings of the WCX World Congress Experience, Detroit, MI, USA, 10–12 April 2018; SAE Technical Paper 2018-01-0228. [CrossRef]
11. Zha, K.; Busch, S.; Warey, A.; Peterson, R.C.; Kurtz, E. A Study of Piston Geometry Effects on Late-Stage Combustion in a Light-Duty Optical Diesel Engine Using Combustion Image Velocimetry. *SAE Int. J. Engines* **2018**, *11*, 783–804. [CrossRef]
12. Perini, F.; Busch, S.; Zha, K.; Reitz, R.; Kurtz, E. Piston Bowl Geometry Effects on Combustion Development in a High-Speed Light-Duty Diesel Engine. In Proceedings of the 14th International Conference on Engines & Vehicles, Naples, Italy, 15–19 September 2019; SAE Technical Paper 2019-24-0167. [CrossRef]
13. Andersson, Ö.; Miles, P.C. Diesel and Diesel LTC Combustion. *Encycl. Automot. Eng.* **2014**, *1*, 1–36. [CrossRef]
14. Eismark, J.; Balthasar, M.; Karlsson, A.; Benham, T.; Christensen, M.; Denbratt, I. Role of Late Soot Oxidation for Low Emission Combustion in a Diffusion-controlled, High-EGR, Heavy Duty Diesel Engine. In Proceedings of the SAE 2009 Powertrains Fuels and Lubricants Meeting, San Antonio, TX, USA, 2–4 November 2009; SAE Technical Paper 2009-01-2813. [CrossRef]
15. Eismark, J.; Balthasar, M. Device for Reducing Emissions in a Vehicle Combustion Engine, Volvo Lastvagnar AB, Göteborg (SE). U.S. Patent 8499735B2, 6 August 2013.
16. Eismark, J.; Andersson, M.; Christensen, M.; Karlsson, A.; Denbratt, I. Role of Piston Bowl Shape to Enhance Late-Cycle Soot Oxidation in Low-Swirl Diesel Combustion. *SAE Int. J. Engines* **2019**, *12*, 233–249. [CrossRef]
17. Zhang, T.; Eismark, J.; Munch, K.; Denbratt, I. Effects of a wave-shaped piston bowl geometry on the performance of heavy duty Diesel engines fueled with alcohols and biodiesel blends. *Renew. Energy* **2019**, *148*, 512–522. [CrossRef]
18. Millo, F.; Piano, A.; Roggio, S.; Bianco, A.; Pesce, F.C. Numerical Investigation on Mixture Formation and Combustion Process of Innovative Piston Bowl Geometries in a Swirl-Supported Light-Duty Diesel Engine. *SAE Int. J. Engines* **2021**, *14*, 247–262. [CrossRef]
19. Dolan, R.; Budde, R.; Schramm, C.; Rezaei, R. 3D Printed Piston for Heavy-Duty Diesel Engines. In Proceedings of the 2018 Ndia Ground Vehicle Systems Engineering and Technology Symposium Power & Mobility (P&M) Technical Session, Novi, MI, USA, 7–9 August 2018. Available online: https://events.esd.org/wp-content/uploads/2018/07/3D-Printed-Piston-for-Heavy-Duty-Diesel-Engines.pdf (accessed on 20 May 2022).
20. Millo, F.; Piano, A.; Roggio, S.; Bianco, A.; Pesce, F.C.; Vassallo, A.L. Numerical Assessment of Additive Manufacturing-Enabled Innovative Piston Bowl Design for a Light-Duty Diesel Engine Achieving Ultra-Low Engine-Out Soot Emissions. *SAE Int. J. Engines* **2021**, *15*, 427–443. [CrossRef]
21. Belgiorno, G.; Boscolo, A.; Dileo, G.; Numidi, F.; Pesce, F.C.; Vassallo, A.; Ianniello, R.; Beatrice, C.; Di Blasio, G. Experimental Study of Additive-Manufacturing-Enabled Innovative Diesel Combustion Bowl Features for Achieving Ultra-Low Emissions and High Efficiency. *SAE Int. J. Adv. Curr. Pract. Mobil.* **2021**, *3*, 672–684. [CrossRef]
22. Millo, F.; Piano, A.; Roggio, S.; Pastor, J.; Micó, C.; Lewiski, F.; Pesce, F.; Vassallo, A.; Bianco, A. Mixture formation and combustion process analysis of an innovative diesel piston bowl design through the synergetic application of numerical and optical techniques. *Fuel* **2021**, *309*, 122144. [CrossRef]
23. Millo, F.; Piano, A.; Peiretti Paradisi, B.; Marzano, M.R.; Bianco, A.; Pesce, F.C. Development and Assessment of an Integrated 1D-3D CFD Codes Coupling Methodology for Diesel Engine Combustion Simulation and Optimization. *Energies* **2020**, *13*, 1612. [CrossRef]
24. Piano, A.; Millo, F.; Boccardo, G.; Rafigh, M.; Gallone, A.; Rimondi, M. Assessment of the Predictive Capabilities of a Combustion Model for a Modern Common Rail Automotive Diesel Engine. In Proceedings of the SAE 2016 World Congress and Exhibition, Detroit, MI, USA, 12–14 April 2016; SAE Technical Paper 2016-01-0547. [CrossRef]
25. Piano, A.; Millo, F.; Postrioti, L.; Biscontini, G.; Cavicchi, A.; Pesce, F.C. Numerical and Experimental Assessment of a Solenoid Common-Rail Injector Operation with Advanced Injection Strategies. *SAE Int. J. Engines* **2016**, *9*, 565–575. [CrossRef]
26. Piano, A.; Boccardo, G.; Millo, F.; Cavicchi, A.; Postrioti, L.; Pesce, F.C. Experimental and Numerical Assessment of Multi-Event Injection Strategies in a Solenoid Common-Rail Injector. *SAE Int. J. Engines* **2017**, *10*, 2129–2140. [CrossRef]
27. Orszag, S.A.; Yakhot, V.; Flannery, W.S.; Boysan, F. Renormalization Group Modeling and Turbulence Simulations. *Near-Wall Turbul. Flows* **1993**, *13*, 1031–1046.
28. Ichards, K.J.; Senecal, P.K.; Pomraning, E. *Converge 2.3 Manual*; Convergent Science Inc.: Madison, WI, USA, 2016.
29. Reitz, R.D.; Bracco, F.V. Mechanisms of Breakup of Round Liquid Jets. *Encycl. Fluid Mech.* **1986**, *3*, 233–249.
30. Amsden, A.A.; O'Rourke, P.J.; Butler, T.D. *KIVA-II: A Computer Program for Chemically Reactive Flows with Sprays*; Los Alamos National Laboratory Technical Report LA-11560-MS; Los Alamos National Lab: Los Alamos, NM, USA, 1989.
31. Schmidt, D.P.; Rutland, C. A New Droplet Collision Algorithm. *J. Comput. Phys.* **2000**, *164*, 62–80. [CrossRef]
32. O'Rourke, P.; Amsden, A. The Tab Method for Numerical Calculation of Spray Droplet Breakup. In Proceedings of the 1987 SAE International Fall Fuels and Lubricants Meeting and Exhibition, Toronto, ON, Canada, 2–5 November 1987; SAE Technical Paper 872089. [CrossRef]

33. O'Rourke, P.; Amsden, A. A Spray/Wall Interaction Submodel for the KIVA-3 Wall Film Model. In Proceedings of the SAE 2000 World Congress, Detroit, MI, USA, 6–9 March 2000; SAE Technical Paper 2000-01-0271. [CrossRef]
34. Zeuch, T.; Moréac, G.; Ahmed, S.S.; Mauss, F. A comprehensive skeletal mechanism for the oxidation of n-heptane generated by chemistry-guided reduction. *Combust. Flame* **2008**, *155*, 651–674. [CrossRef]
35. Frenklach, M.; Wang, H. Detailed modeling of soot particle nucleation and growth. *Symp. Int. Combust.* **1991**, *23*, 1559–1566. [CrossRef]
36. Kazakov, A.; Wang, H.; Frenklach, M. Detailed modeling of soot formation in laminar premixed ethylene flames at a pressure of 10 bar. *Combust. Flame* **1995**, *100*, 111–120. [CrossRef]
37. Kazakov, A.; Frenklach, M. Dynamic Modeling of Soot Particle Coagulation and Aggregation: Implementation with the Method of Moments and Application to High-Pressure Laminar Premixed Flames. *Combust. Flame* **1998**, *114*, 484–501. [CrossRef]